

Dependence of the $^{12}\text{C}(\vec{\gamma}, pd)$ reaction on photon linear polarisation

D.P. Watts^{a,*}, J.R.M. Annand^a, R. Beck^b, D. Branford^c, D.I. Glazier^{a,1}, P. Grabmayr^d,
K. Livingston^a, I.J.D. MacGregor^a, J.C. McGeorge^a, R.O. Owens^a, G. Rosner^a

^a Department of Physics and Astronomy, University of Glasgow, Glasgow, G12 8QQ, UK

^b Institut für Kernphysik, Universität Mainz, D-55099 Mainz, Germany

^c School of Physics, University of Edinburgh, Edinburgh, EH9 3JZ, UK

^d Physikalisches Institut, Universität Tübingen, D-72076 Tübingen, Germany

Received 22 June 2006; received in revised form 6 December 2006; accepted 7 February 2007

Available online 15 February 2007

Editor: V. Metag

Abstract

The sensitivity of the $^{12}\text{C}(\vec{\gamma}, pd)$ reaction to photon linear polarisation has been determined at MAMI, giving the first measurement of the reaction for a nucleus heavier than ^3He . Photon asymmetries and cross sections were measured for $E_\gamma = 170$ to 350 MeV. For E_γ below the Δ resonance, reactions leaving the residual ^9Be near its ground state show a positive asymmetry of up to 0.3, similar to that observed for ^3He suggesting a similar reaction mechanism for the two nuclei.

© 2007 Elsevier B.V. All rights reserved.

PACS: 21.30.Fe; 25.20.Ij; 27.20.+n

The study of photon induced proton–deuteron knockout from nuclei may give valuable information on the three-body interaction in the nucleus, since the direct mechanisms which contribute are related to those thought to be involved [1–4] in the three-nucleon force (3NF). Gaining sensitivity to 3NFs in photon induced knockout reactions is particularly desirable as it should give access to the short-range aspects of forces in the nucleus, as already evidenced in studies of the nucleon–nucleon force [5]. In addition to the basic $^3\text{He}(\gamma, pd)$ reaction, it is also important to study the (γ, pd) reaction in heavier nuclei which have more typical nuclear density and in which a wider range of relative angular momentum and spin couplings can contribute.

As well as the direct 3-nucleon knockout mechanism there are expected to be contributions from additional mechanisms such as initial photon absorption by a single nucleon (1N), by two-nucleons (2N) and also two-step 3N processes such as initial real pion production on one nucleon followed by reabsorp-

tion by a nucleon pair. Clearly, to extract reliable information from experimental data the relative contributions from each of these mechanisms should be well understood. In particular, measurements of the photon asymmetry are expected to be of utility as it has been shown for various photonuclear reactions that at low missing energies the asymmetry is only weakly influenced by distortions of the outgoing particle wavefunctions by the nuclear potential [6,7]. The photon asymmetries presented here will provide an additional tool to investigate the mechanisms contributing to the (γ, pd) reaction from nuclei for a range of photon energies (E_γ) and in different excitation energy regions of the (A–3) nucleus.

There has been significant theoretical interest in the (γ, pd) reaction in recent years. Detailed ^3He calculations based on exact solutions of the three-nucleon scattering equations in the initial and final states have recently become available [1,3]. The modelling of the photon coupling includes a realistic treatment of both π - and ρ -like meson exchange currents. For E_γ regions where free pion production is unimportant these models give an exact description of the reaction dynamics from the basic nuclear forces. Predictions have been made up to $E_\gamma \sim 240$ MeV in this Faddeev scheme [1] which show that the inclusion of a

* Corresponding author.

E-mail address: dwatts1@ph.ed.ac.uk (D.P. Watts).

¹ Present address: School of Physics, University of Edinburgh, UK.

3NF has large effects, increasing the predicted magnitude of the cross section by up to $\sim 100\%$ at $E_\gamma \sim 120$ MeV. Very recently the calculations have been extended to predict the photon asymmetry [8] and the inclusion of 3NFs was shown to increase the asymmetry by up to $\sim 35\%$.

A microscopic theoretical treatment of the ${}^3\text{He}(\gamma, pd)$ reaction based on a diagrammatic approach which includes contributions from 1N, 2N and 3N mechanisms and which does include the free pion degree of freedom has been developed by Laget [4]. The inclusion of the additional channels was carried out with the penalty of employing a factorisation approximation to simplify the integrations in the calculation. Although less exact than the treatment of Refs. [1,3] the inclusion of the extra channels means the model is applicable up to $E_\gamma \sim 500$ MeV. Unfortunately no asymmetry calculations have been carried out and so the interpretation of the $(\vec{\gamma}, pd)$ data over a wider energy range using the Laget calculation is not presently possible.

On the experimental side, most measurements of the (γ, pd) reaction have been made using ${}^3\text{He}$ targets [9,10]. An important feature of the measured excitation functions is that they show no structure for photon energies in the $\Delta(1232)$ resonance region. The ${}^3\text{He}(\gamma, pd)$ proton angle distributions are moderately well described by the Laget model when 1N, 2N and two-step 3N (including only real π exchange) mechanisms are included [4,9]. Above ~ 150 MeV the two-step 3N mechanism is predicted to provide most of the cross section for centre-of-mass (CM) proton angles backwards of $\sim 70^\circ$. The ${}^3\text{He}(\gamma, pd)$ data at deuteron laboratory angles of 90° and 110° have also been compared to the Faddeev calculations of the process, which are seen to give a fairly good description of the cross section, even up to $E_\gamma \sim 240$ MeV [1].

The only previous (γ, pd) cross sections measured in $A > 3$ nuclei were for ${}^{16}\text{O}$ [11] and ${}^{12}\text{C}$ [12] and no photon asymmetry measurements have been obtained. Both measurements show a photon energy dependence similar to that observed in ${}^3\text{He}$ with no prominent enhancement for E_γ around the Δ resonance. This behaviour is in contrast to photon induced pp , pn , $p\pi$ and ppn [13–16] knockout reactions where the Δ plays a prominent role. The ${}^{12}\text{C}(\gamma, pd)$ missing energy spectra obtained in Ref. [12] exhibit significant strength close to the reaction threshold, and the recoil momentum spectra of the $(A-3)$ nucleus at low missing energies are consistent with those predicted if it were a spectator to the knockout of three $1p$ -shell nucleons.

The photon asymmetry for the $(\vec{\gamma}, pd)$ reaction has only been measured previously for ${}^3\text{He}$ [17,18]. These measurements showed a positive asymmetry which ranged from around 0.2 to 0.5 over the sampled photon energy region of 90–350 MeV and CM proton angle range of 60 – 135° . The Faddeev calculations [8] reproduce the asymmetry at $E_\gamma \sim 120$ MeV but show a tendency to underestimate the asymmetry of the higher E_γ data. In all cases 3NFs move the predicted asymmetries closer to the data.

The three nucleon photoabsorption mechanisms which operate in the (γ, pd) reaction also contribute in the (γ, ppn) reaction but with less restrictive spin and isospin conditions for the final state particles [15,19]. Recent Faddeev calcula-

tions for ${}^3\text{He}$ [1,2] indicate that the (γ, ppn) reaction is also sensitive to the nature of the 3NF. Several measurements of the ${}^3\text{He}(\gamma, ppn)$ reaction have been made in the last decade [15, 20,21] which suggest that the largest contribution arises from two-step 3N mechanisms involving the exchange of an on-shell meson. The same conclusion was obtained from a study of the ${}^{12}\text{C}(\gamma, ppn)$ reaction [16] but clear evidence for the existence of a direct 3N mode was also presented.

The present work is the first measurement of the ${}^{12}\text{C}(\vec{\gamma}, pd)$ reaction. The experiment was carried out at the 855 MeV Mainz microtron (MAMI-B) [22] using the Glasgow tagged-photon spectrometer [23,24] in conjunction with two plastic scintillator arrays, PiP and TOF [25,26], set up as described in Ref. [27,28]. Polarised photons were produced by coherent bremsstrahlung in a thin diamond radiator [29,30]. The polarisation orientation of the photons was flipped between horizontal and vertical every few minutes. Three angular settings of the diamond were used for which the main coherent peak covered the photon energy ranges 170–220, 220–280 and 300–350 MeV with corresponding average linear polarisation (P) of 59.5%, 49.5% and 42.5% respectively.

Protons with kinetic energies 31–270 MeV were detected in the charged particle hodoscope PiP covering the polar angular range $\theta = 51^\circ$ – 129° and azimuthal angular range of $\phi = \pm 23^\circ$. Coincident deuterons leaving the target with energies above ~ 45 MeV were detected in TOF which determined particle energies by time-of-flight. The TOF detectors covered $\theta = 10.0^\circ$ – 175.0° with a uniform ϕ acceptance of 13.5° to -18.0° set by a software cut. The deuterons were separated from other charged hadrons in TOF by selecting events from a 2-D plot of inverse speed versus pulse height, as described in Ref. [12]. The number of random deuteron coincidences in TOF was found to be negligible. The average measured missing energy resolution extracted from $\text{D}(\gamma, pn)$ was found to be ~ 7 MeV. For (γ, pd) the average resolution is better due to the slower flight times for the heavier particles and is estimated to be ~ 5 MeV. The $\sim 3\%$ background of events not originating from reactions in the target was measured in runs with the target removed. The total systematic error in the asymmetry is estimated to be $\Delta\Sigma = \pm 0.05\Sigma$ [27]. The systematic uncertainties in the measured cross sections are estimated to be up to $\pm 8\%$ [12].

For each goniometer setting all events due to photons in the coherent peak region were used to produce average $(\vec{\gamma}, pd)$ cross sections (σ) and asymmetries (Σ) for the events which were within the geometrical and energy acceptances of the PiP-TOF detector systems. The asymmetry is defined as $\Sigma = \frac{1}{P} \frac{\sigma^\parallel - \sigma^\perp}{\sigma^\parallel + \sigma^\perp}$ where σ^\parallel (σ^\perp) is the measured cross section for reactions in which the horizontal detector plane is parallel (perpendicular) to the electric vector of the polarised photons. The reduction of Σ due to integrating the $\cos(2\phi)$ dependence of the asymmetry over the finite experimental ϕ acceptance and including a correction for the effects of Fermi momentum is estimated to be $\sim 10\%$. The magnitude of the presented asymmetries have been increased by this factor to account for this. The effect on the asymmetry due to smearing of the photon polarisation direction in the $(3N + \gamma)$ CM frame by the ini-

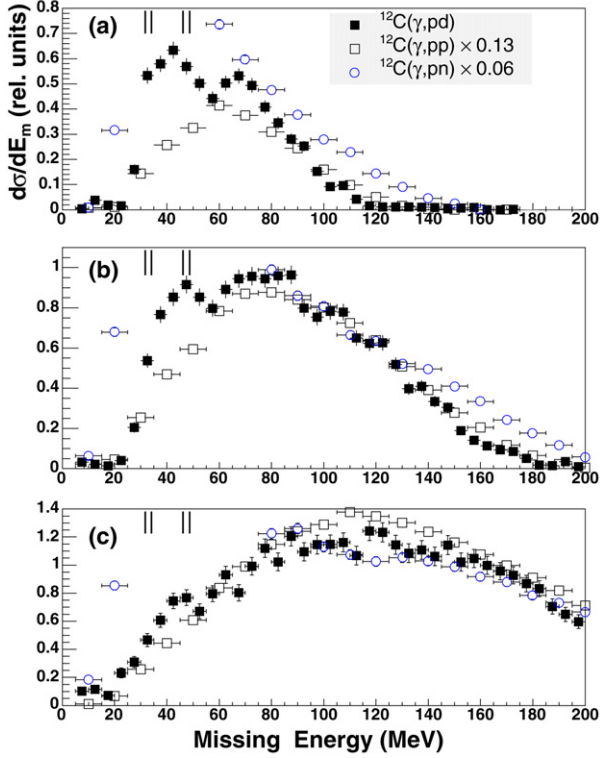


Fig. 1. Cross sections for the (γ, pd) , (γ, pp) and (γ, pn) reactions versus missing energy are shown as the filled squares, open squares and open circles, respectively. The data are presented for E_γ bins of (a) 170–220 MeV, (b) 220–280 MeV and (c) 280–350 MeV. The (γ, pp) and (γ, pn) cross sections have been scaled by the factors indicated on the figure. The ground state and the three narrow excited states in ${}^9\text{Be}$ at 2.4, 14.4 and 17.0 MeV are indicated by the marks on the top of each panel.

tial $3N$ Fermi momentum is estimated to be $\sim 0.5\%$ and is neglected.

The cross section as a function of E_m is shown in Fig. 1 for three different E_γ bins. Missing energy is defined as $E_m = E_\gamma - T_1 - T_2 - T_r$ where E_γ is the incident photon energy, T_1 and T_2 are the energies of the two detected particles and T_r is the (typically small) energy of the recoiling system which is calculated from its momentum $\mathbf{P}_r = \mathbf{P}_\gamma - \mathbf{P}_1 - \mathbf{P}_2$. The (γ, pd) missing energy spectra rise rapidly above the threshold at $E_m = 31.7$ MeV and reach a maximum for $E_m \sim 45$ MeV. The rise is sharpest and the maximum most pronounced for the lowest E_γ bin for which the energy resolution is best and the underlying background is smallest. At higher E_m the (γ, pd) missing energy distributions all rise to a second maximum, which becomes higher and wider as E_γ increases. Similar features are seen in the earlier work of Ref. [12], but less pronounced due to its poorer statistical accuracy and inferior resolution. A (γ, pd) reaction which involves the knockout of three ($1p$) shell nucleons leaving a residual ($A-3$) spectator would populate missing energies up to ~ 50 MeV and this suggests that much of the observed strength in this region can be attributed to such a spectator process as indicated in Ref. [12]. Also shown in Fig. 1 are the scaled ${}^{12}\text{C}(\gamma, pp)$ and ${}^{12}\text{C}(\gamma, pn)$ cross sections obtained with the same detector setup as the present measurement (these data were already

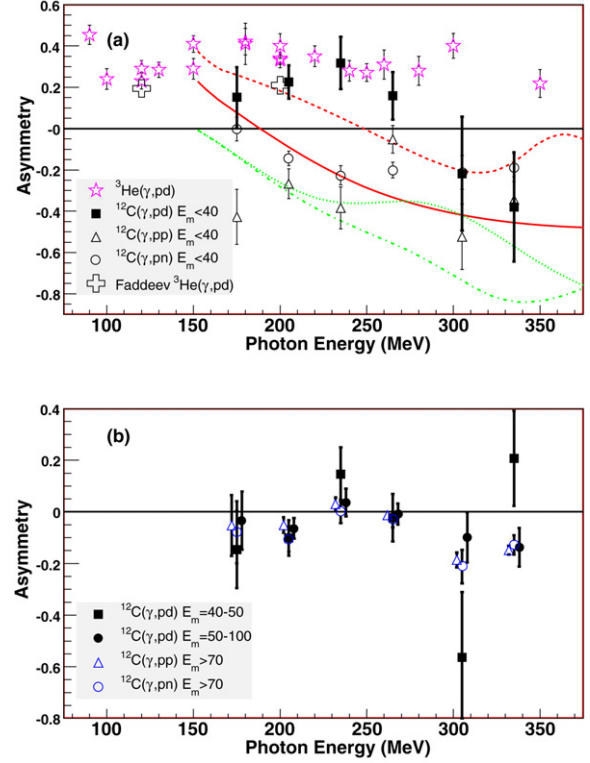


Fig. 2. (a) The ${}^{12}\text{C}(\vec{\gamma}, pd)$, ${}^{12}\text{C}(\vec{\gamma}, pn)$ and ${}^{12}\text{C}(\vec{\gamma}, pp)$ photon asymmetry integrated over $\theta_p = 51^\circ$ – 120° for the missing energy cuts indicated in the figure. The errors shown are statistical only. The experimental results [17] for ${}^3\text{He}(\vec{\gamma}, pd)$ at $\theta_p = 90^\circ$ and 110° and the Faddeev predictions [8] at $\theta_p = 110^\circ$ are also shown. The red (solid) and green (dot-dash) lines give the asymmetry at $\theta_\pi = 55^\circ$ from the MAID calculations for $p(\vec{\gamma}, \pi^0)p$ and $p(\vec{\gamma}, \pi^+)n$ respectively. The corresponding predictions without including the $\Delta(1232)$ are shown by the red (dashed) and green (dotted) lines. (b) Comparison of the ${}^{12}\text{C}(\vec{\gamma}, pd)$, ${}^{12}\text{C}(\vec{\gamma}, pn)$ and ${}^{12}\text{C}(\vec{\gamma}, pp)$ asymmetry at higher missing energy.

analysed in Ref. [27]). Above $E_m \sim 60$ MeV the (γ, NN) reactions scale with E_m and E_γ in a similar way to the present ${}^{12}\text{C}(\gamma, pd)$ data. At low E_m the channels show different behaviour. The peak observed at $E_m \sim 45$ MeV in the (γ, pd) data is absent in the (γ, pp) data and the (γ, pn) cross section has a large peak at $E_m \sim 30$ MeV (off scale in Fig. 1) due to a large direct two-nucleon knockout contribution.

The photon asymmetry for the ${}^{12}\text{C}(\vec{\gamma}, pd)$ reaction is presented in Fig. 2. The $E_m < 40$ MeV region emphasises (γ, pd) reactions leading to the ground state and low lying excited states of ${}^9\text{Be}$. A positive asymmetry is observed for photon energies up to $E_\gamma \sim 280$ MeV, while at higher photon energies in the Δ resonance region the asymmetry becomes negative. The asymmetry for ${}^3\text{He}(\vec{\gamma}, pd)$ for $\theta_p = 90$ and 110° in the CM frame [17] (both corresponding to lab proton angles covered by the PiP detector in the present measurement) are also shown in Fig. 2(a). The magnitude and sign of the ${}^3\text{He}$ asymmetry is similar to the $E_m < 40$ MeV ${}^{12}\text{C}$ data for photon energies up to ~ 270 MeV. At higher E_γ the ${}^3\text{He}$ data do not show the negative or small asymmetries indicated in the ${}^{12}\text{C}(\vec{\gamma}, pd)$ data.

The $E_m = 40$ – 50 MeV cut (Fig. 2(b)) emphasises ($1p$)³ knockout events leading to higher excited states and includes

the peak region visible in the cross section as a function of missing energy (Fig. 1). The asymmetry in this region is generally negative or small below ~ 300 MeV in contrast to the positive asymmetry observed at lower missing energies for both ^{12}C and $^3\text{He}(\vec{\gamma}, pd)$. The asymmetry for the $E_m = 50\text{--}100$ MeV region shows the same general trends as the $E_m = 40\text{--}50$ MeV data, albeit smaller in magnitude. The asymmetries for both these higher E_m regions can be seen to show features which are very similar to those observed for the $^{12}\text{C}(\vec{\gamma}, NN)$ reactions at high missing energy [27], suggestive of similar underlying reaction mechanisms. The model of Ref. [19] explains the (γ, NN) cross section in this missing energy region largely as the result of detecting two of the three (or more) nucleons produced by a two-step 3N process or by initial photon absorption on a two-nucleon pair followed by final state interactions [31,32]. The same processes, where one of the outgoing nucleons picks up an additional nucleon from the residual nucleus, can probably explain the similar E_m distribution and asymmetry of the $^{12}\text{C}(\vec{\gamma}, pd)$ reaction. As these mechanisms involve more than three nucleons they have no analogue in the reaction on ^3He .

A comparison of the (γ, pp) and (γ, pd) E_m distributions below 60 MeV may suggest the pickup process discussed in the previous paragraph still provides a significant background contribution in this region. However, this extrapolation should be considered an upper limit since at low E_m the dominant mechanism of the (γ, pp) reaction changes to direct two-proton emission following photon absorption on two-nucleons [31, 32], which only has significant subsequent pickup probability at more forward proton angles than sampled here [4]. This is supported by the comparison in Fig. 2 of the $^{12}\text{C}(\vec{\gamma}, pd)$ asymmetry with the asymmetry of the $^{12}\text{C}(\vec{\gamma}, pp)$, and $^{12}\text{C}(\vec{\gamma}, pn)$ reactions for $E_m \leq 40$ MeV [27]. Both the reactions show a negative asymmetry. The positive asymmetries observed in $^{12}\text{C}(\vec{\gamma}, pd)$ therefore argue against a large direct feeding of strength from (γ, pp) and (γ, pn) reactions through subsequent pickup reactions at the lowest missing energies.

The selection of $^{12}\text{C}(\vec{\gamma}, pd)$ events with low missing energy should enhance the contribution of processes which involve only the three detected nucleons while the (A–3) nucleus spectates. The asymmetry observed for the $(\vec{\gamma}, pd)$ reaction in ^3He and for ^{12}C in this E_m region (Fig. 2(a)) suggests similar reaction mechanisms in both nuclei. The recent Faddeev predictions [8] presented in the figure can be seen to give a fair account of the measured asymmetry for $^3\text{He}(\vec{\gamma}, pd)$ without including the real pion degree of freedom. However, as the Laget model predicts that the two-step 3N mechanism involving the initial production of a real pion is the dominant mechanism at the higher E_γ sampled in the present experiment it is interesting to assess the contribution of this mechanism to the asymmetry. Laget [4] does not calculate the $^3\text{He}(\vec{\gamma}, pd)$ asymmetry, but an indication of its behaviour is sought here by examining the asymmetry in the initial $p(\vec{\gamma}, N)\pi$ stage of the dominant 3N two-step mechanism. Since the (γ, pd) process involves deuteron formation from the recoiling nucleon in this initial process, then the underlying $(\vec{\gamma}, N)\pi$ asymmetry may be reflected in the $(\vec{\gamma}, pd)$ data as was already observed in the $(\vec{\gamma}, NN)$ measurements [27] at high missing energy.

To examine this the $\vec{\gamma}N \rightarrow N\pi$ asymmetry was obtained using the MAID code [33]. Both $p(\vec{\gamma}, \pi^+)n$ and $p(\vec{\gamma}, \pi^0)p$ were calculated at a pion CM breakup angle of 55° , which for photon energies above 200 MeV results in recoiling nucleon angles in regions where the deuteron yield in the present $^{12}\text{C}(\vec{\gamma}, pd)$ data is largest ($\sim 40\text{--}60^\circ$). The predictions are presented in Fig. 2(a). Neither of the full $p(\vec{\gamma}, \pi)N$ calculations can give a simple explanation of the low missing energy $^{12}\text{C}(\vec{\gamma}, pd)$ asymmetry. As the Δ contribution to the initial pion production vertex for the two-step 3N process is suppressed due to an isospin restriction [4], MAID calculations with the Δ contribution removed are also shown in Fig. 2. While the $p(\vec{\gamma}, \pi^0)p$ MAID prediction with no Δ contribution comes closer to the $(\vec{\gamma}, pd)$ asymmetry, the MAID cross sections are largest for the $p(\gamma, \pi^+)n$ process for which the asymmetry is negative. It therefore seems unlikely that the asymmetries for $^{12}\text{C}(\vec{\gamma}, pd)$ at low missing energy or for $^3\text{He}(\vec{\gamma}, pd)$ can be reproduced with this simple interpretation of the two-step 3N mechanism.

In summary this first determination of the $^{12}\text{C}(\vec{\gamma}, pd)$ asymmetry shows that reactions leading to low lying states in ^9Be proceed through the photon interacting with the detected nucleons in a similar manner to $^3\text{He}(\vec{\gamma}, pd)$ for E_γ below the Δ resonance. As the asymmetry in ^3He is predicted by exact Faddeev calculations to be sensitive to the inclusion of 3NFs, these first $^{12}\text{C}(\vec{\gamma}, pd)$ results suggest a possible new route to access 3NFs in the (1p) shell. The asymmetries at higher missing energy do not resemble $^3\text{He}(\vec{\gamma}, pd)$ and have a plausible explanation in terms of multistep processes involving more than three nucleons. These new results will provide valuable constraints on the reaction mechanisms for (γ, pd) in heavier nuclei and their potential to be used in learning about the correlated behaviour of three nucleons in a nucleus. Future work with improved statistical accuracy and with a range extending below the π production threshold would be a desirable next step and could be achieved at high flux facilities such as the laser backscattering facility at Duke University [34].

Acknowledgements

This work was supported by the UK EPSRC, the British Council, the DFG (Mu 705/3, SSP 1043), BMFT (06 Tu 656), DAAD (313-ARC-IX-95/41), the EC [SCI.0910.C(JR)] and NATO (CRG 970268).

References

- [1] R. Skibinski, et al., Phys. Rev. C 67 (2003) 054001.
- [2] R. Skibinski, et al., Phys. Rev. C 67 (2003) 054002.
- [3] A. Deltuva, et al., Phys. Rev. C 70 (2004) 034004.
- [4] J.M. Laget, Phys. Rev. C 38 (1988) 2993.
- [5] C. Giusti, et al., Eur. Phys. J. A 26 (2005) 209.
- [6] J. Ryckebusch, D. Debruyne, W. Van Nespen, Phys. Rev. C 57 (1998) 1319.
- [7] F.X. Lee, et al., Phys. Rev. C 60 (1999) 034605.
- [8] R. Skibinski, et al., Phys. Rev. C 72 (2005) 044002.
- [9] V. Isbert, et al., Nucl. Phys. A 578 (1994) 525.
- [10] N. Kolb, et al., Phys. Rev. C 49 (1994) 2586.

- [11] H. Hartmann et al., in: Proceedings of the International Conference on Photonuclear Reactions and Applications, Asilomar, CA, USA, Lawrence Livermore Lab. Conf. No. 730301, 1973, p. 967, unpublished.
- [12] S.J. McAllister, et al., Phys. Rev. C 60 (1999) 044610.
- [13] I.J.D. MacGregor, et al., Phys. Rev. Lett. 80 (1998) 245.
- [14] D. Branford, et al., Phys. Rev. C 61 (2000) 014603.
- [15] G. Audit, et al., Nucl. Phys. A 614 (1997) 461.
- [16] D.P. Watts, et al., Phys. Lett. B 553 (2003) 25.
- [17] A.A. Belyaev, et al., JETP Lett. 40 (1984) 1275.
- [18] F.L. Fabbri, et al., Lett. Nuovo Cimento 3 (1972) 63.
- [19] R.C. Carrasco, M.J. Vicente Vacas, E. Oset, Nucl. Phys. A 570 (1994) 701.
- [20] C. Ruth, et al., Phys. Rev. Lett. 72 (1994) 617.
- [21] A. Sarty, et al., Phys. Rev. C 47 (1993) 459.
- [22] T. Walcher, Prog. Part. Nucl. Phys. 24 (1990) 189.
- [23] I. Anthony, et al., Nucl. Instrum. Methods A 301 (1991) 230.
- [24] S.J. Hall, et al., Nucl. Instrum. Methods A 368 (1996) 698.
- [25] I.J.D. MacGregor, et al., Nucl. Instrum. Methods A 382 (1996) 479.
- [26] P. Grabmayr, et al., Nucl. Instrum. Methods A 402 (1998) 85.
- [27] C.J.Y. Powrie, et al., Phys. Rev. C 64 (2001) 034602.
- [28] S. Franczuk, et al., Phys. Lett. B 450 (1999) 332.
- [29] F. Rambo, et al., Phys. Rev. C 58 (1998) 489.
- [30] F. Natter, et al., Nucl. Instrum. Methods B 211 (2003) 465.
- [31] T. Lamparter, et al., Z. Phys. A 355 (1996) 1.
- [32] D.P. Watts, et al., Phys. Rev. C 62 (2000) 014616.
- [33] D. Drechsel, et al., Nucl. Phys. A 645 (1999) 145.
- [34] H.R. Weller, M.W. Ahmed, Mod. Phys. Lett. A 18 (2003) 1569.